Comparison of the power balance in a Totem-Pole Bridgeless PFC topology with several inrush current limiting strategies

Sebastien Jacques, Cedric Reymond, Jean-Charles Le Bunetel, Ghafour Benabdelaziz

Journal of ELECTRICAL ENGINEERING, VOL 72(2021), NO1, 12–19

sciendo

PAPERS

Comparison of the power balance in a Totem-Pole Bridgeless PFC topology with several inrush current limiting strategies

Sébastien Jacques[1*], Cédric Reymond[1,2], Jean-Charles Le Bunetel[1], Ghafour Benabdelaziz[2]

Limiting inrush currents is usually necessary when AC-DC conversion is used to supply DC loads such as battery chargers in particular, it must comply with IEC 61000-3-3. This document discusses the suitability of an active inrush current limiter that can be used to replace traditional thermistors and NTC relays. This strategy is based on the control of the phase shift of thyristor type power components. It has been implemented in a totem-pole bridgeless power factor corrector (PFC). Experimental results show that this solution differs from traditional solutions to ensure high energy efficiency (higher than 95%) while limiting inrush currents.

K e y w o r d s: totem-pole-bridgeless PFC topology, inrush current limitation, control of the phase shift of thyristor

1 Introduction

In recent years, numerous research activities have promoted the use of electric vehicles (EVs) to support the power grid to become more efficient and ensure a balance between electricity production and consumption. In particular, the battery reserves of EVs can help balance the grid and provide electrical power, especially during peak consumption periods. A key element of this strategy is the battery charger that converts AC to DC power [1, 2].

Power Factor Correction (PFC) topologies are today widely used in AC-DC conversion [3]. Most of these topologies use a bridge rectifier and a Boost converter. However, this type of structure induces many losses due to voltage drops in both the rectifier stage and the Boost converter. In this article, a Totem-Pole Bridgeless PFC topology (see Fig. 1) is chosen to increase the efficiency of the AC-DC conversion. Although this type of structure is well described in the literature, the reverse recovery charges in the body diodes of power MOSFETs at each switching period do not allow it to operate properly. With SiC and GaN power devices (see S_1 and S_2 in Fig. 1), this topology becomes more and more attractive [4, 5]. To further increase the energy performance of this structure, the slow diodes (see D_1 and D_2 in Fig. 1) can also be replaced by two Si MOSFETs (S_3 and S_4) making the converter fully bidirectional (see Fig. 2). In this case, the literature indicates that the energy efficiency of such a structure can reach 99 %, which is 3 % higher than traditional PFC topologies [6, 7].

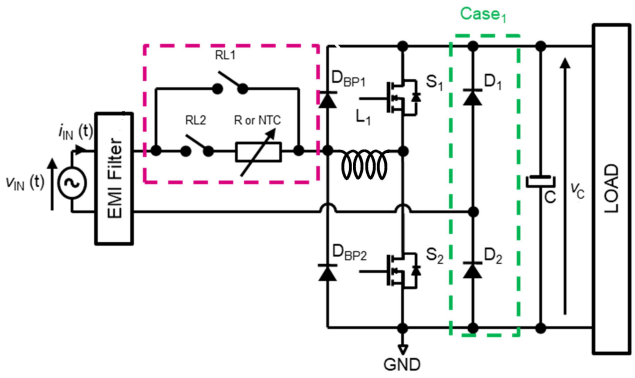

Fig. 1. Example of a totem-pole bridgeless PFC topology that implements a passive inrush current limitation consisting of a thermistor, relays and diodes

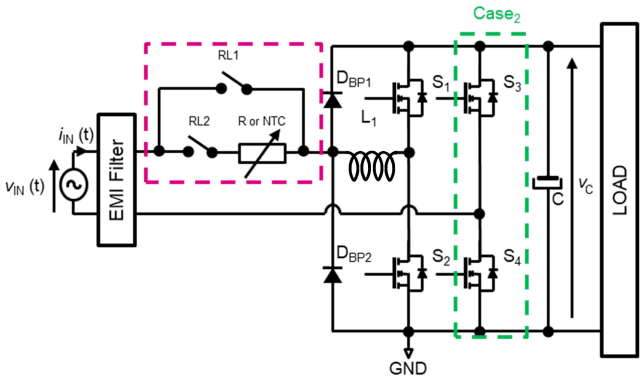

Fig. 2. Example of a totem-pole-bridgeless PFC topology that implements a passive inrush current limitation consisting of a thermistor, relays and MOSFETs

[1] University of Tours, GREMAN UMR 7347, CNRS, INSA Centre Val-de-Loire, Tours 37100, France, [2] Application and System Engineering, STMicroelectronics Tours SAS, Tours 37000, France, *Correspondence: sebastien.jacques@univ-tours.fr

DOI:10.2478/jee-2021-0002, Print (till 2015) ISSN 1335-3632, On-line ISSN 1339-309X

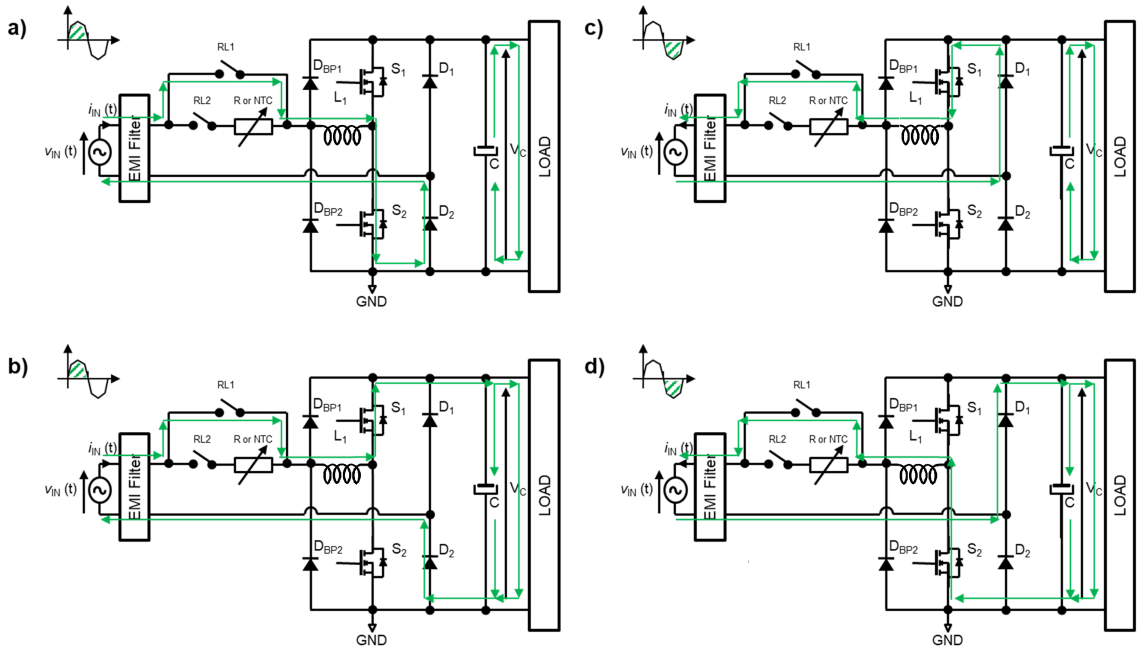

Fig. 3. Operating phases of the totem-pole-bridgeless PFC topology: during the positive half cycle of the AC grid voltage (a) – $\forall t \in [0\,; dTs]$, (b) – $\forall t \in [dTs\,; Ts]$, and during the negative half cycle of the AC grid voltage (c) – $\forall t \in [0\,; dTs]$, (d) – $\forall t \in [dTs\,; Ts]$

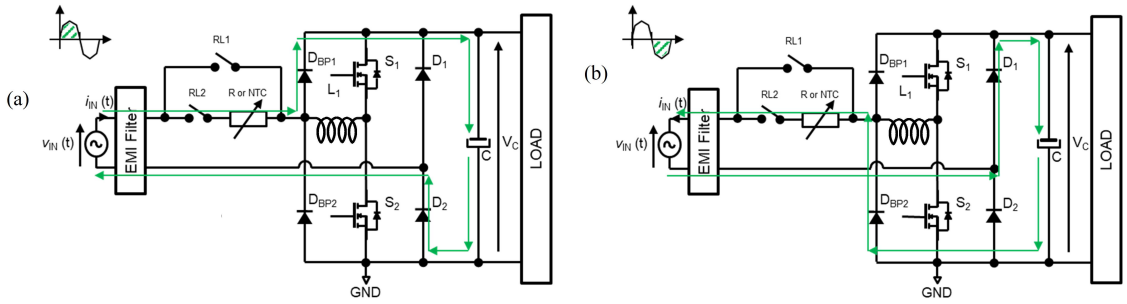

Fig. 4. Inrush current path with traditional solution when the AC-DC converter is connected according to the AC line polarity (a) – positive half cycle, (b) – negative half cycle

Figure 3 gives the operating phases of the Totem-Pole Bridgeless PFC topology. In the following discussion, two parameters are specified the operating period named Ts and the duty cycle named d. During the positive half cycle of the AC grid voltage, there are two phases. During the time interval between 0 and dTs, see Fig. 3(a), S_2 is ON, S_1 is OFF and D_2 is ON. The inductor is charging, and the output capacitor supplies the DC bus. Over the time interval between dTs and Ts, see Fig. 3(b), S_2 is OFF, the body diode inside S_1 is ON, and D_2 is always ON. The energy stored in the inductor supplies the DC bus. The proposed topology is totally symmetrical. Thus, in the same way as above, during the negative half cycle of the AC grid voltage, two phases can also be described. During the time interval between 0 and dTs, see Fig. 3(c), S_1 is ON, S_2 is OFF and D_1 is ON. The inductor is charging and the output capacitor supplies the DC bus. During the time interval between dTs and Ts, see Fig. 3(d), S_1 is turn OFF, the body diode inside S_2 is ON and D_1 is always ON. The energy stored in the inductor supplies the DC bus.

Many current AC-DC power supplies require a large output capacitor also called bulk capacitor (*ie*, $1\,\mu$F/W with a 230 V RMS power supply) connected to the DC bus. This capacitor acts as an energy storage unit. When the AC-DC converter is plugged into the AC grid, a high current spike appears and charges the bulk capacitor to the peak value of the AC voltage [8, 9]. This transient phenomenon can reduce the reliability of the converter. Therefore, an inrush current limiting strategy is necessary.

As shown in Fig. 4, most inrush current limiting strategies use a negative temperature coefficient (NTC) thermistor (or resistor) in series with the output bulk capacitor [10]. Figure 4 shows the operating phases of the proposed totem-pole-bridgeless PFC topology during converter start-up. For the positive line cycle of the AC grid, the current flows through the limiting component (resis-

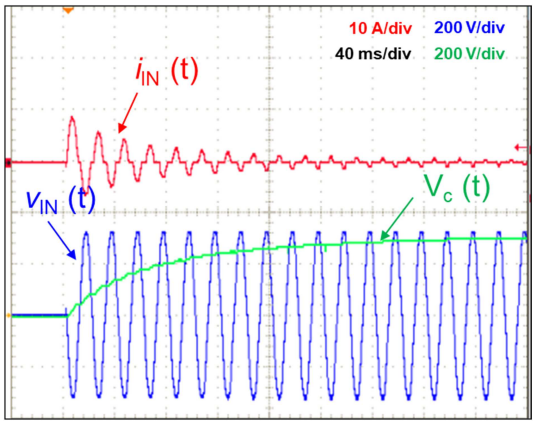

Fig. 5. Soft-start experimental waveforms with NTC and relay in the totem-pole-bridgeless PFC topology experimental conditions: $R = 35\,\mathrm{m\Omega}$, $C = 1$ mF $V_{in} = 230$ V RMS, $F = 50$ Hz

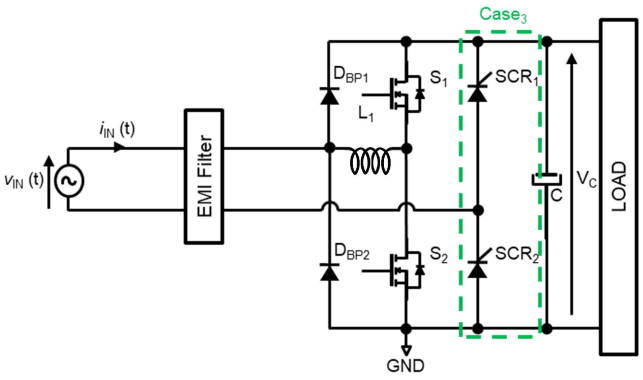

Fig. 6. Proposal of a totem-pole-bridgeless PFC topology based on thyristors

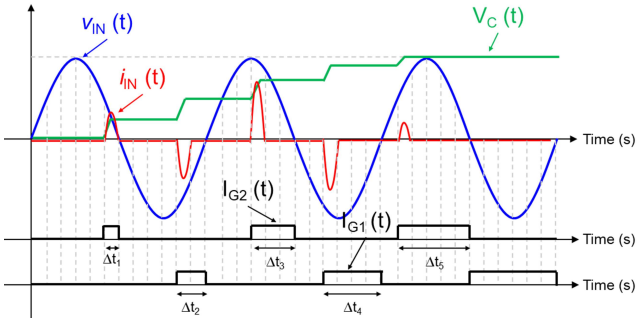

Fig. 7. The concept of thyristor phase shift control

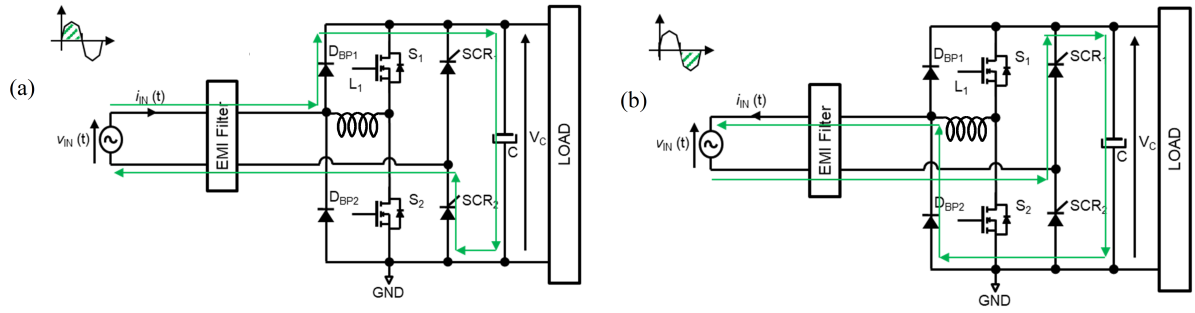

Fig. 8. Inrush current path with thyristor solution when the ACDC converter is connected according to the AC line polarity (a) – positive half cycle, (b) – negative half cycle

tor or thermistor) and then through the bypass diode D_{BP1} to charge the bulk capacitor. Then, the current returns to the AC grid through D_2 . During the negative line cycle of the AC grid, the current charge the bulk capacitor through D_1 . Then, the current returns to the AC grid through the bypass diode D_{BP2} and the limitation component (resistor or thermistor). When the capacitor is charged, the thermistor (or resistor) is shunted by an electromechanical relay (R_{L1}), in particular to reduce power losses in steady state. The DC bus can also be disconnected using an additional relay (R_{L2}) to ensure low standby power consumption. Figure 5 shows the typical waveforms of a soft start with this type of solution.

Electromechanical relays in AC-DC converters do not offer optimal solutions for limiting inrush currents, as they have many disadvantages [11, 12]. Indeed, this type of solution is cumbersome. In addition, it requires powering the relay coil. This solution is also sensitive to vibrations. An explosion can occur, especially in flammable environments. Finally, this traditional solution does not manage the AC grid and a high current can damage electronic devices, blow the input fuse, decrease the reliability of the system, *etc*.

This paper proposes to demonstrate the relevance of a thyristor-based active inrush current limiting strategy,

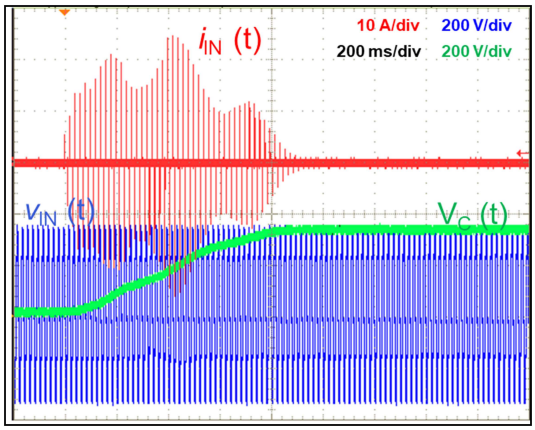

Fig. 9. Soft-start experimental waveforms by adjusting the thyristor turn on delay experimental conditions: $C = 1\,\text{mF}$, $V_{\text{in}} = 230\,\text{V}$ (RMS), $F = 50\,\text{Hz}$, $\Delta t = 50\,\mu\text{s}$

which is implemented in a bridgeless PFC totem and the power balance inside the converter is analyzed.

Section 2 explains the thyristor-based active inrush current limiting strategy. In the last section, the efficiency of the power converter with the traditional and proposed inrush current limiting strategy is discussed. This discussion is based on the complete results of experimental measurements.

2 Theoretical analysis: active inrush current limiters based on thyristors

To limit inrush currents while avoiding the disadvantages described in the first section of the article, the thermistor (or resistor) and relays (see Fig. 1) must be removed. The slow diodes (see D_1 and D_2 in Fig. 1) can also be replaced by two thyristors to reduce power losses (see Fig. 6). It is important to note that this solution can be implemented in all AC-DC converters.

As shown in Fig. 7, the output bulk capacitor can be progressively charged by controlling the phase shift of the thyristors. In particular, SCR_1 and SCR_2 are alternately activated with a delay (Δt) depending on the polarity of the AC grid. This delay increases gradually until the voltage across the bulk capacitor reaches the peak value of the AC grid voltage. As long as the thyristors are not controlled, the rectifier bridge cannot conduct any current. Thus, the output bulk capacitor cannot be charged. This solution is very interesting because it reduces standby power consumption by disconnecting the DC bus.

As can be seen in Fig. 8(a), during the positive half cycle of the AC grid voltage, the inrush current flows through the bypass diode named D_{BP1}, charges the bulk output capacitor named C and returns to the AC grid through the thyristor named SCR_2. During the negative half cycle of the AC grid voltage, see Fig. 8(b), the inrush current flows through SCR_1, charges the C-capacitor and returns to the AC grid through the bypass diode named D_{BP2}.

Figure 9 shows the voltage development across the bulk capacitor during the start-up of the proposed totem-pole-bridgeless PFC topology implementing a soft start procedure which is controlled by the phase shift delay of the thyristors. Regarding battery chargers, the start-up duration allowed to charge the output bulk capacitor must be lower than one second. According to the results described in Fig. 9, the charging time of the output bulk capacitor is about 850 ms. In this case, the transient current can reach 11 A (peak value). This strategy is particularly useful for compliance with IEC 61000-3-3, as the RMS value of the transient current is less than 16 A. Remember that IEC 61000-3-3 is applicable to electrical and electronic systems with an input current equal to or less than 16 A per phase, intended to be connected to public low-voltage distributions (between 220 V and 250 V line to neutral at 50 Hz). This is indeed the case for the applications described in this article.

3 Experimental results and discussion

3.1 Optimization of the energy efficiency

In this section of the paper, the objective is to optimize the steady-state energy efficiency of the proposed totem-pole-bridgeless PFC topology that implements an inrush current limiting strategy. The methodology is based on the choice of semiconductor device technologies to achieve the best efficiency of the entire converter. Three configurations are proposed here for comparison. The following analysis is based on two main assumptions. The first assumes that the nominal power of the AC-DC converter is equal to 3.7 kW (the AC grid voltage is equal to 230 V RMS). The second assumes that the power losses are estimated in the worst case (*ie* at 150 °C) for an RMS input current equal to 16 A.

As shown in Fig. 1, the first case (see Case 1) involves the use of two slow diodes coupled to an electromechanical relay implemented in the totem-pole-bridgeless PFC topology. The second case (see Fig. 1, Case 2) uses two silicon MOSFETs instead of slow diodes. The third case (see Fig. 6, Case 3) uses two thyristors instead of silicon MOSFETs. Furthermore, in this case, the electromechanical relay is removed.

For the first case (see Fig. 1, Case 1), two diode technologies are compared. The first is the ultra-fast diode which has a fast charge recovery time (*ie* $t_{rr} = 50$ ns). This type of diode is usually implemented in a high-frequency switching cell. In this study, the switching frequency is very low (*ie* 50 Hz). Therefore, this type of diode technology is generally not chosen. The second uses the very low conduction loss diode which has a low dynamic resistance (*ie* $R_d = 4\,\text{m}\Omega$). This kind of diode technology is typically implemented in a rectifier bridge. Fig. 10 shows the evolution of the forward current (I_F) as a function of the forward voltage (V_F) for these two

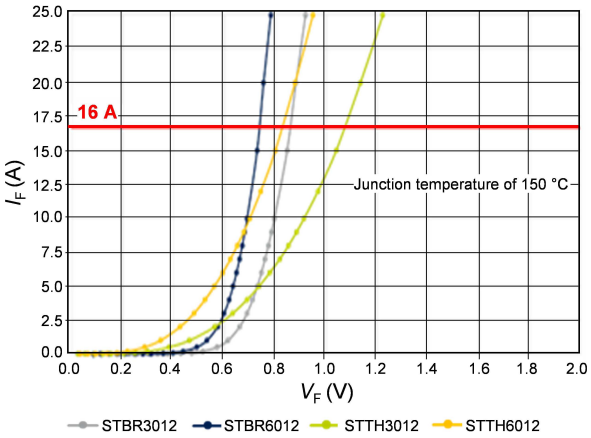

Fig. 10. Evolution of the forward current (I_F) depending on the forward voltage (V_F). Comparison of 4 diode technologies: STTH3012 (1.200 V ultrafast recovery diode), STTH6012 (1, 200 V ultrafast recovery diode), STBR3012 (1, 200 V diode with ultra-low conduction losses), and STBR6012 (1, 200 V diode with ultra-low conduction losses) [experimental results]

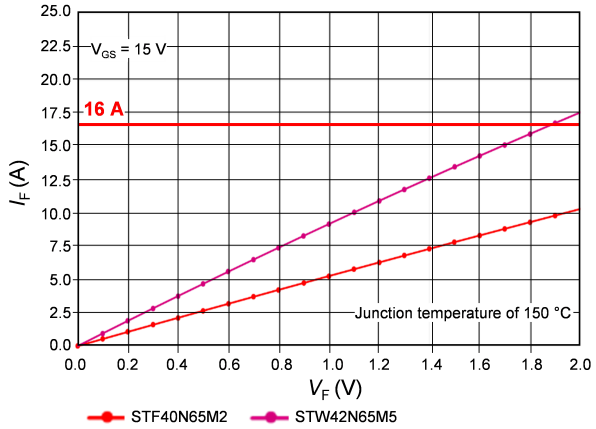

Fig. 11. Evolution of the forward current (I_F) depending on the forward voltage (V_F). Comparison of 2 MOSFETs' technologies: STF40N65M2 (2^{nd} generation MDmesh^{TM} technology) and STW42N65M5 (5^{th} generation MDmesh^{TM} technology) [experimental results]

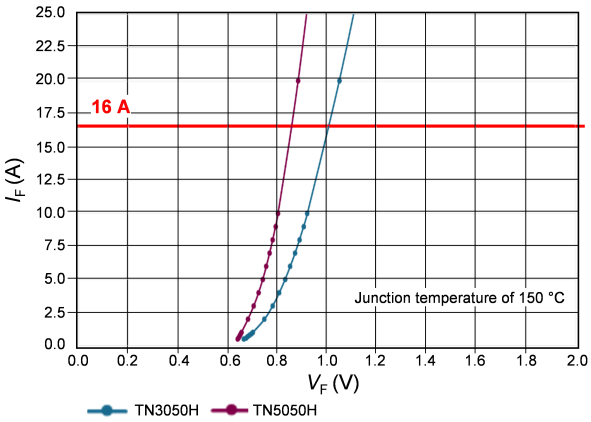

Fig. 12. Evolution of the forward current I_F depending on the forward voltage V_F in the first quadrant comparison between TN3050H and TN5050H thyristors experimental results

diode technologies. This characteristic is of utmost importance for selecting the diode technology that has both the lowest values of voltage drop and dynamic resistance to minimize losses during steady-state operation.

From Fig. 10, for the same value of the forward current, the higher the voltage rating of the diode, the lower the V_F-value. For a forward current lower than 9 A (reference: STxx3012) and 4 A (reference: STxx6012), the power losses of the ultrafast recovery diodes (*ie* STTH3012 and STTH6012) are lower than ultra-low conduction losses diodes (*ie* STBR3012 and STBR6012). However, regarding the targeted application, the diode technology must be chosen depending on the current (*ie* in that case, 16 A RMS). Finally, the most important parameter is the V_F-value at a forward current value equal to 16 A RMS. Fig. 10 highlights that the V_F-value of the STBR6012 diode is about 0.73 V. In that case, the conduction losses equal 6 W. Therefore, diodes with very low conduction losses are well suited in this study.

Regarding the second case (see Fig. 1, Case 2) which uses a silicon MOSFET coupled with an electromechanical relay, the study focuses on the MDMesh^{TM} technology, and particularly the second generation (M2) and the fifth generation (M5). Figure 11 shows the evolution of the forward current depending on the forward voltage. The performances of two semiconductor devices are particularly compared: STF40N65M2 (N-channel MOSFET; 650 V, 87 mΩ, 32 A MDmesh^{TM} M2 technology) and STW42N65M5 (N-channel MOSFET; 650 V, 70 mΩ, 33 A MDmesh^{TM} M5 technology). The on-state resistance ($R_{DS(ON)}$) of the STW42N65M5 MOSFET (*ie*, 108 mΩ at 150 °C) is lower than the STF40N65M2 MOSFET (*ie*, 190 mΩ at 150 °C). So, the fifth generation of MDmesh^{TM} technology offers low conduction losses compared with the second generation of MDmesh^{TM} MOSFET. It is important to note that the V_F-value of the fifth generation of MDmesh^{TM} MOSFET is equal to 1.72 V for a drain-to-source current equal to 16 A RMS.

Regarding the third case (see Fig. 6, Case 3) which consists in replacing the silicon MOSFETs, STMicroelectronics has recently developed two thyristors: the TN3050H (30 A, 1, 200 V thyristor) and the TN5050H (50 A, 1, 200 V thyristor) which both are dedicated to automotive applications. For these two thyristors, Fig. 12 shows the evolution of forward current depending on the forward voltage in the first quadrant.

As with diodes, the higher the voltage rating of the SCR, the larger the silicon die and the lower the V_F-value. Thus, with an RMS current value of 16 A, the TN3050H and TN5050H thyristors give V_F-values of 0.95 V and 0.85 V respectively, resulting in conduction losses of 8.4 W in the worst case (*ie* at a junction temperature of 150 °C).

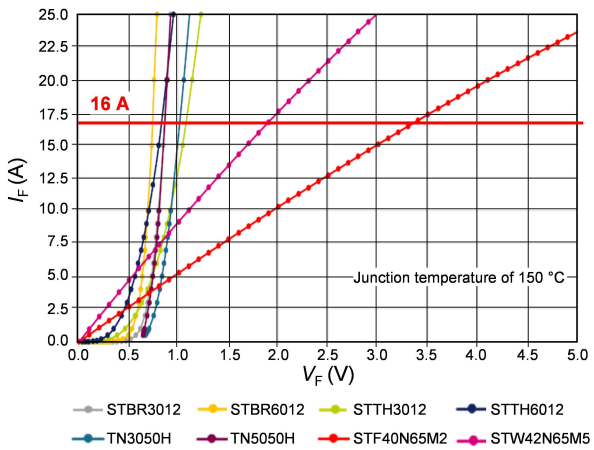

Fig. 13. $I_F(V_F)$ characteristics in the first quadrant comparison of the solutions without any electromechanical relay experimental measurement results

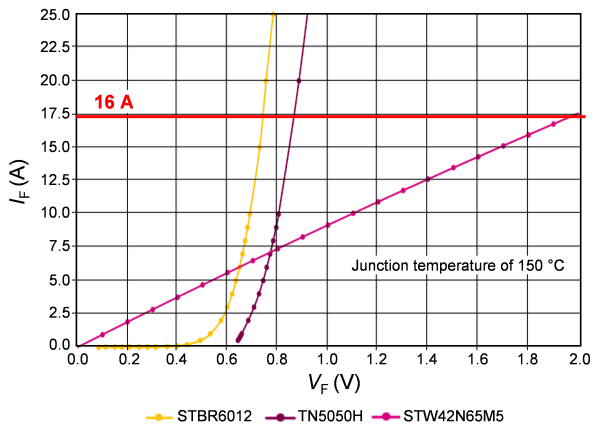

Fig. 14. $I_F(V_F)$ characteristics in the first quadrant comparison of the solutions with the electromechanical relay experimental results

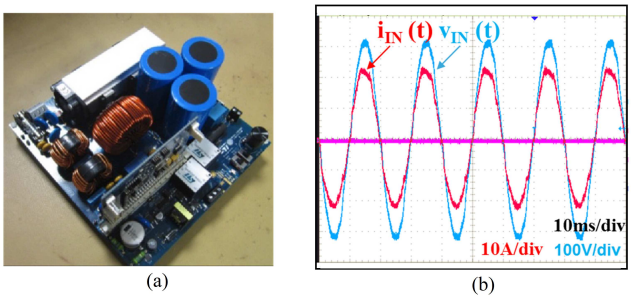

Fig. 15. (a) – prototype of the 3.7 kW totem-pole-bridgeless PFC topology (b) – examples of waveforms during the steady state operation

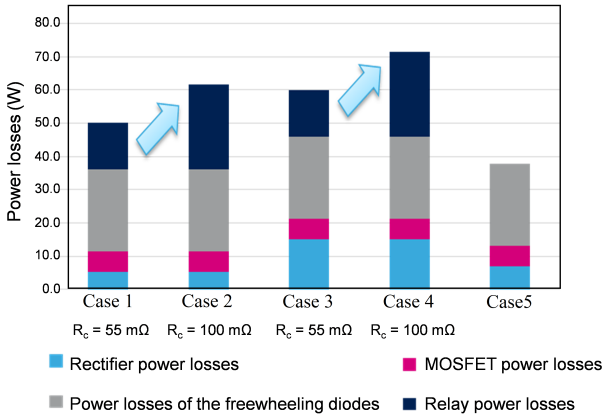

Fig. 16. Comparison of power losses for the solutions studied

Figure 13 shows a comparison of the $I_F(V_F)$ characteristics (Q1) for the three solutions described above.

The characteristics of the TN5050H thyristor correspond to those of the STBR3012 diode. The STTH6012 diode has a voltage drop (V_F) equal to 0.81 V, *ie* 40 mV less than that of the TN5050H thyristor.

However, in order to better compare all the solutions, it is necessary to take into account the voltage drop of the electromechanical relay in addition to the static characteristic, especially for the second solution (see Fig. 1, Case 2) and the last one (see Fig. 6, Case 3). The device used (reference: OMIH-SH-112 LM) in this application is a 16 A relay which is composed of a contact of AgSnO type and a 16 A rating. Figure 14 shows a comparison of the three solutions taking into account the characteristics of the electromechanical relay. When direct current values are below 5 A, diodes with very low conduction power losses (especially the STBR6012 diode) coupled to an electromechanical relay have a low voltage drop in the conducting state compared to that of the thyristor TN5050H. However, when the forward current values are high, the thyristors have a lower voltage drop. To conclude this analysis, the thyristor-based solution (see Fig. 6, Case 3) should be chosen to optimize the energy efficiency of the AC-DC converter.

3.2 Comparison of steady-state power losses

Figure 15 shows the prototype of the 3.7 kW totem-pole-bridgeless PFC topology used to characterize its energy efficiency taking into account the results of the analysis described in the previous section. Figure 15 also shows some examples of steady-state waveforms.

The overall conduction losses are evaluated when the 3.7 kW AC-DC converter is connected to the 230 V RMS, 50 Hz AC grid. Figure 16 shows the distribution of the overall power losses for the three solutions described in the previous section of the paper.

With the first solution (see Fig. 1, Case 1) which uses diodes coupled to a thermistor (or a resistor) and an electromechanical relay, the global losses (*ie* conduction losses and switching power losses) inside the AC-DC converter reach 50.25 W. With the second solution (see Fig. 1, Case 2) which uses MOSFETs coupled to a thermistor (or a resistor) and an electromechanical relay, the global losses are equal to 59.98 W. In these two cases, the power losses due to the relay are equal to 14 W. The contact resistance of the relay is equal to 55 mΩ.

However, to have a much more complete comparison, it is necessary to take into account the evolution of the contact resistance of the relay according to the number

Table 1. Summary of the energy efficiency of the totem-pole-bridgeless PFC topology with several inrush current limiting strategies

	Advantages	Drawbacks	Ranking of Solutions according to energy efficiency
Case 1	- No auxiliary power supply - Cost	- Does not manage the AC grid dropout - High bulk density - Increase of the relay contact resistance with the number of operating cycles → increase of the power losses - Losses due to the coil consumption	2nd
Case 2	- Bidirectional converter	Does not manage the AC grid dropout - High bulk density - Increase of the relay contact resistance with the number of operating cycles → increase of the power losses - Losses due to the coil consumption - Need of an auxiliary power supply and an insulated control circuit	3rd
Case 3	- Manage the AC grid dropout - High inrush current accuracy - Low bulk density	- Need of an auxiliary power supply and an insulated control circuit	1st

of operating cycles [13]. The data sheet of the electromechanical relay gives a contact resistance of 100 mΩ. In this case, the power losses due to the relay are equal to 25.5 W (both for Case 1 and Case 2). This value is therefore higher than the value of 14 W characterized in the previous paragraph.

The last solution with thyristors (see Fig. 6, Case 3) shows the best experimental results. Indeed, the overall losses inside the AC-DC converter are about 37.9 W. These losses do not change with the number of cycles compared to traditional solutions (see Fig. 1, Case 1 and Case 2). Table 1 summarizes the advantages and disadvantages of each solution. The first solution (see Fig. 1, Case 1) has a major advantage: it is easier to implement because it does not require any auxiliary power supply or additional control circuitry. The second solution (see Fig. 1, Case 2) may be useful if the application requires bidirectional current to transfer electrical energy from the battery to the AC grid. The last thyristor-based solution (see Fig. 6, Case 3) is different from the other solutions in that it is more energy efficient and can better manage inrush currents.

4 Conclusion

In this article, a relevant solution has been proposed and implemented to limit inrush currents when an AC-DC converter is connected to the AC network. This solution is based on thyristor phase angle control.

This active inrush current limiter has been implemented in a totem-pole-bridgeless PFC topology. It has been compared to two other solutions currently deployed in many industrial applications: the first is based on a thermistor (or a resistor) coupled with an electromechanical relay and two diodes; the second uses a thermistor (or a resistor) coupled with an electromechanical relay and two MOSFETs.

All solutions have been evaluated in terms of energy efficiency through a comprehensive experimental test procedure. The results underline that the thyristor-based solution stands out from the others, both in terms of high energy efficiency and good inrush current management. In addition, this solution is well suited to reduce standby power consumption. Finally, the robustness of such a solution can be increased.

References

[1] S.-W. Choi, Y.-J. Kim, and J.-Y. Lee, "Design of 10 kW Three-Phase EV Charger with Wide Output Voltage Range Based on Voltage-Fed Isolated PFC Converter", *EPE Journal*, vol. 29, no. 1, pp. 11–24, 2018.

[2] B. Chauchat, S. Bacha,M. Brunello, and J.-P. Ferrieux, "Three-Phase Battery Charger for Electric Vehicle", *EPE Journal*, vol. 9, no. 1-2, pp. 60–65, 1999.

[3] Ch. Andrieu, J.-P. Ferrieux, and M. Rocher, "The AC-DC Stage: A Survey of Structures and Chopper Control Modes for Power Factor Correction", *EPE Journal*, vol. 9, no. 3-4, pp. 17–22, 1996.

[4] B. Su, J. Zhang, and Z. Lu, "Totem-Pole Boost Bridgeless PFC Rectifier with Simple Zero Current Detection and Full-Range

ZVS Operating at Boundary of DCM/CCM", *IEEE Transaction on Power Electronics*, vol. 26, no. 2, pp. 427–435, 2011.

[5] Q. Huang, "Review of GaN Totem-Pole-Bridgeless PFC", *CPSS Transactions on Power Electronics and Applications*, vol. 2, no.3, pp. 187–196, 2017.

[6] M. Bharathidasan, "Review of Power Factor Correction (PFC) AC/DC-DC Power Electronic Converters for Electric Vehicle Applications", *IOP Conference Series: Materials Science and Engineering*, vol. 906, 012006, 2020.

[7] L. Zhou and Y. Wu, *99% Efficiency True-Bridgeless Totem-pole PFC Based on GaN HEMTs*, Transphorm USA, 2015.

[8] G. Rajalakshmi, R. Ashok Kumar, and K. Asokan, "Power Factor Improvement of Buck-Boost AC-DC Converter using Pulse Width Modulation Strategy", *International Journal of Computer Sciences and Engineering*, vol. 6, no. 11, pp. 158–163, 2018.

[9] T. Ghanbari, "Thyristor Based Bridge-Type Fault Current Limiter for Fault Current Limiting Capability Enhancement", *IET Generation, Transmission & Distribution*, vol. 10, no. 9, pp. 2202–2215, 2016.

[10] API Technologies Corp., *l Inrush current limiting NTC Thermistors*, Power Electronics Technology, 2013.

[11] C. Reymond, S. Jacques,G. Benabdelaziz, and J-C. Le Bunetel, "An Active Inrush Current Limiter Based on SCR Phase Shift Control for EV Charging Systems", *Journal of Energy and Power Engineering*, vol. 10, no. 4, pp. 247–257, 2018.

[12] S. Jacques, N. Batut, R. Leroy, and L. Gonthier, "Aging Test Results for High Temperature TRIACs During Power Cycling", In: *Proceedings of the 2008 IEEE Annual Power Electronics Specialists Conference* (PESC), Rhodes, Greece, pp. 2447–2452, 2008.

[13] B. Renard, *Smart Inrush Current Limiter Enables Higher Efficiency AC/DC converters*, HOW2POWER TODAY, 2016, http://www.how2power.com/article/2016/may/smart-inrush-current-limiter-enables-higher-efficiency-in-ac-dc-converters.php.

Received 17 December 2020

Sébastien Jacques received the PhD degree in electrical engineering from the University of Tours, France, in 2010. Since 2012, he has been with the Research Group on Materials, Microelectronics, Acoustics and Nanotechnologies (GREMAN UMR 7347, CNRS, INSA Centre Val-de-Loire), where he has been hired as an Associate Professor. His current research interests include power converters, electricity management in smart buildings, machine learning and reliability of electronic systems.

Cédric Reymond received his Master degree in electrical engineering from Joseph Fourier University of Grenoble, France in 2015. He received the PhD degree in electrical engineering from the University of Tours, France, in 2019. His main area of interest is power electronics (*ie* static converters, modeling and control).

Jean-Charles Le Bunetel received the PhD degree in electrical engineering from the University of Le Havre, France, in 1997. He is currently a full Professor at the University of Tours, France. He is with the research group on materials, microelectronics, acoustics and nanotechnology (GREMAN UMR 7347, CNRS, INSA Centre Val-de-Loire). His research interests include power electronics, converter structures, electromagnetic interference modeling and associated electromagnetic compatibility problems.

Ghafour Benabdelaziz received the PhD degree in electrical engineering from the University of Tours, France, in 2005. He is currently working at STMicroelectronics Tours SAS and particularly, within the Application and System Engineering laboratory. His major fields of interest include power electronics (*ie* static converters, modelling and control, transformers), digital electronics (*ie* microcontrollers) and power semiconductor devices (*ie* thyristors, Triacs).